Competing Tenure

The Intersection of Forests, Food, and Fuel at Indonesia's National Strategic Project in Merauke, South Papua

May 2026

Technical Appendix

1. SAR and Landsat Classification

This study focuses on a defined geographic region in Papua, Indonesia, delineated using a custom buffered shapefile that included sugarcane concession parcels and the surrounding area. We selected this area to assess and evaluate forest loss occurring within the concession boundaries and the areas adjacent to the formal concession boundaries. We conducted analysis for two time periods, representing pre- and post-periods. For the former, the date range was August 1, 2023 through June 1, 2024. For the latter, the range was May 1, 2025 through May 20, 2025. These dates were chosen to capture post-monsoonal vegetative conditions while minimizing the influence of seasonal anomalies.

For the pre-period, we conducted a supervised land cover classification using optical imagery from Landsat 8 and Landsat 9 Surface Reflectance Collections (Collection 2, Tier 1) provided by the United States Geographical Survey and accessed via Google Earth Engine (GEE). Concurrently, we integrated Synthetic Aperture Radar (SAR) imagery from Sentinel-1, characterized by dual-polarization (VV and VH) data and descending orbital passes, to enhance classification accuracy, especially under the conditions of persistent cloud cover that are typical in tropical environments.[1] The SAR imagery in the post-period conditions were particularly necessary given widespread and consistent cloud cover in the available Landsat imagery.

To ensure high-quality optical imagery, we implemented a pixel quality-based cloud masking approach. This method effectively masked out clouds and cloud shadows, retaining only clear-sky pixels across the visible, near-infared (NIR), and short-wave infrared (RED) spectral bands. We generated a median composite of cloud-masked imagery to provide a stable and representative dataset for classification. Additionally, we computed the Normalized Difference Vegetation Index (NDVI) using the formula (NIR - RED) / (NIR + RED). The NDVI provided a quantitative measure of vegetation health and density, significantly aiding differentiation among agricultural land, natural vegetation, and other land cover classes.

We processed SAR imagery to leverage its all-weather imaging capabilities, a crucial strategy for classifying vegetation in tropical regions, mosaicking Sentinel-1 imagery, specifically VV and VH polarization bands, for the study period. To mitigate the inherent speckle noise, we applied a focal

mean filter with a 30-meter radius circular kernel, thus enhancing the interpretability for surface features. Additionally, we calculated the polarization difference (VV - VH), which is effective for discerning surface roughness and land cover types with distinct structural characteristics. To further refine classification accuracy, we extracted textural features from SAR data using the Gray-Level Co-Occurrence Matrix (GLCM) method with a 3x3 pixel window. Specifically, we selected contrast and entropy metrics from both VV and VH polarization bands. These texture metrics provided additional insight into the structural and spatial properties of land surfaces, notably improving the differentiation of agricultural land from naturally vegetated areas.

We defined ten land cover classes based on visual interpretation of Landsat imagery, RGB composite of SAR imagery, and previous studies in the region: open water, flooded vegetation, palm plantations, forest, savanna, shrubland, rice paddies, agriculture, infrastructure, and bare earth. We manually digitized polygons representing these classes, using them as training samples for the supervised classification.

Table 1. Land cover characteristics for classification.

Class Name	Optical Characteristics	SAR Characteristics	Key Feature
Open Water	Very low reflectance across all bands, especially NDVI and SWIR.	Very low backscatter, appearing as smooth dark patches in both VV and VH.	Stable dark tone in both Landsat and SAR imagery.
Flooded Vegetation	Mixed spectral signature; vegetation with moderate NDVI.	Stronger double-bounce scattering in VH polarization compared to open water, producing bright textures around water-vegetation interfaces.	Bright VH backscatter and partial vegetation NDVI.
Palm Plantations	High NDVI values; structured, repeating canopy patterns visible in Landsat composites.	Regular texture with high VV backscatter, moderate VH.	High structural regularity and periodic texture in SAR imagery.
Forest	High NDVI values; dense green tones in Landsat composites.	Strong volume scattering, especially high VH backscatter.	Bright, noisy VH texture and consistent NDVI.
Savanna	Moderate NDVI.	Moderate VV and VH backscatter; texture more open.	Heterogenous patches of vegetation with mixed backscatter.
Shrubland	Low to moderate NDVI; shrubs visible as patchy cover.	Moderate backscatter; rough texture without canopy volume scattering.	Intermediate backscatter and patchy NDVI.
Rice Paddies	Bright NDVI in growth stages and dark appearance of flooded stages.	Rectangular parcel patterns detectable; low backscatter from flooded paddies, higher VH returns from growing rice.	Geometric parcel boundaries.

Agriculture	Moderate to high NDVI.	Variable backscatter, less consistent than palm or rice; geometric parcel boundaries.	Distinct human-modified textures; geometric pattern of fields.
Infrastructure	Very bright in visible bands, low NDVI.	Very high backscatter (especially VV); bright stable patches.	High VV backscatter, sharp edges.
Bare Earth	High reflectance in visible bands, low NDVI.	Moderate VV backscatter, lower VH; texture smooth but brighter than water.	Low vegetation indices, medium SAR returns, homogenous patches.

Using the composite dataset comprising optical spectral bands, NDVI, SAR polarimetric bands, and GLCM-derived texture features, we trained a Random Forest classifier implemented in GEE, selecting the Random Forest method due to its robustness in handling multi-dimensional data and resistance to overfitting, thereby enhancing classification accuracy. The resulting classified image provided a high-resolution thematic land cover map at a 30-meter spatial resolution.

For the post-period, persistent and widespread cloud cover prevented the use of Landsat imagery for land cover classification. Instead, we relied exclusively on SAR imagery from Sentinel-1 to detect landcover change. We assembled mosaics of dual-polarization (VV and VH) SAR imagery from 2024 and 2025, applying a focal mean filter with a 30-meter radius kernel to reduce speckle noise. To quantify vegetation change, we calculated the difference in backscatter between the two periods across both polarizations. We applied a statistical threshold, defining significant change as pixels with values greater than two standard deviations from the mean difference. This thresholding approach isolated areas of pronounced vegetation loss.[2]

We then used this binary change mask to extract the affected areas from the pre-period land cover classification. In effect, the mask overlaid the 2024 classification to identify where transitions from vegetated classes had occurred due to vegetation loss. This approach, combined with a previously-constructed 23-class land cover map,[3] enabled us to assess the spatial extent of forest conversion while overcoming the limitations posed by persistent cloud cover in the post-period.

2. Protest Data

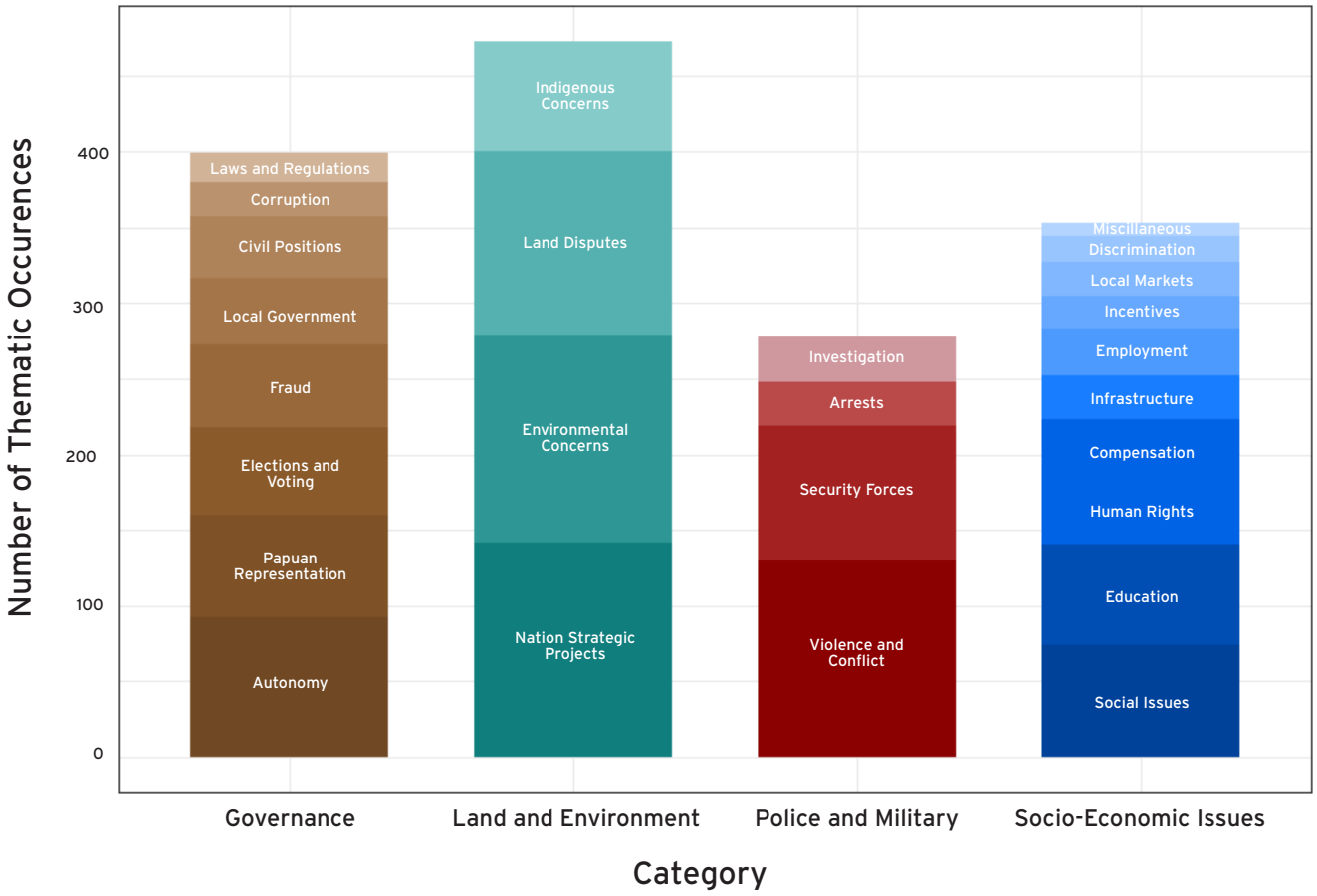

Figure 1: Issues raised at protests in Papuan provinces between January 2020-July 2025.

3. Land Use Scenarios

We tested a range of land use scenarios, based upon mapping from the Ministry of Investment[4] and mapping reported by Nusantara Atlas.[5] For the former, we georeferenced mapping to create shapefiles representing the Cluster III Planning Area identified by the Ministry of Investment. Within GOI documentation, land cover is reported for concessions and buffer zones connecting them. When considering overlap by land cover type, our mapping and the GOI's mapping correspond tightly, particularly in the case of forest cover.

Table 2. Land cover area by source, and difference between sources.

Land Cover	Reported Area, Including Buffer Zones (ha)		Difference	Reported Area, No Buffer Zones (ha)
	GOI	CGS		CGS
Primary Dryland Forest	201,967	173,648	15.08%	172,111
Degraded Dryland Forest	167,292	195,711	-15.66%	180,300
Primary Mangrove Forest	295	173	52.05%	173
Degraded Mangrove Forest	490	595	-19.43%	595
Primary Peat Swamp Forest	39,789	40,923	-2.81%	38,928
Degraded Peat Swamp Forest	42,675	38,462	10.39%	27,928
Forest Plantation	0	3,582	-200.00%	1,042
Forest	452,507	453,094	-0.13%	420,390
Shrub	10,523	16,470	-44.07	13,300
Wetland Shrub	0	37,370	-200.00%	28.238
Swamp	48,668	48,477	-0.39%	39,814
Savana	67,915	41,623	48.01%	30,410
Grasslands, Wetlands, & Shrub	127,106	143,940	-12.42%	111,762
Agriculture	7,080	850	157.13%	572
Dry Cultivation	2,646	2,665	-0.71%	2,634
Mixed Cultivation & Shrub	1,582	9,297	-141.82%	8,376
Rice	536	615	-13.78	68
Palm	0	11,511	-200.00%	11,511
Agriculture	11,844	24,938	-71.20%	23,161
Settlement	684	399	52.68%	289
Transmigration	7,612	1,246	143.73%	1,077
Bare Land	8,608	2,516	109.53%	1,923
Water	29,059	926	187.65%	858
Other	45,963	5,087	160.14%	4,147
Total	**637,420**	**627,059**	**1.64%**	**559,460**

For the latter, we created a range of scenarios based upon sugarcane production efficiency, in tons of cane per hectare. After determining land required, based upon each efficiency scenario, we determined the share of mapped sugarcane concessions required to meet each scenario, using buffers to add or subtract area from baseline concessions.

Table 3. Sugarcane land use scenarios and mapping methodologies.

Scenario	Sugarcane Efficiency (tc/ha)	Land Required (Kha)	ArcGIS Land Selection Methodology
Low Efficiency	58	1,521.5	All area within mapped sugarcane concessions, removing non-arable land classes (settlements, transmigration areas, port & harbor, open water, mining areas) + Buffer, removing non-arable land classes
Average Historical Efficiency	67	1,321.6	All area within mapped sugarcane concessions, removing non-arable land classes + Buffer, removing non-arable land classes
High Efficiency	80	1,102.9	Mapped sugarcane concessions with observed GLAD-L forest loss alerts within their boundaries[6] + Concessions bordering those with observed forest loss
Presidential Regulation No. 40/2023 Efficiency	93	950.6	Mapped sugarcane concessions with observed GLAD-L forest loss alerts within their boundaries[6] + Inset buffer

Figure 2: Area included in each land use scenario a. Low efficiency **b.** Average historical efficiency **c.** High efficiency **d.** Presidential Regulation No. 40/2023 efficiency

4. Emissions Calculations

4.1 Land Clearing Emissions

Equation One. Emissions from clearing for sugarcane plantations.

$$E_{Clearing} = (GHG_{LUC} \times CF \times A) \pm (GHG_{LUC} \times U \times CF \times A)$$

$E_{Clearing}$ = emissions from clearing for sugarcane plantations ($MtCO_2e$)

GHG_{LUC} = one-time GHG emissions from aboveground and belowground carbon stock ($MgC\ ha^{-1}$)

CF = the conversion factor for converting carbon into CO_2e, set at 3.67

A = total area converted (ha)

U = uncertainty percentage

Table 4. Emissions factors for AGB and BGB in Papua by land cover type.

Land Cover Class	Emissions Factor, MgC ha^{-1}	Uncertainty, %	Land Cover Class	Emissions Factor, MgC ha^{-1}	Uncertainty, %
Primary Dryland Forest	346.45	0.054	Open Water	0	0
Secondary Dryland Forest	289.95	0.078	Wet Shrub	23.91	0.3342
Primary Mangrove Forest	315.48	0.182	Pure Dry Agriculture	16.89	0.911
Primary Swamp Forest	271.9	0.151	Mixed Cultivation & Shrub	77.56	0.0593
Secondary Mangrove Forest	167.39	0.104	Rice	12.36	0.6327
Secondary Swamp Forest	170.65	0.165	Fish Pond	0	0
Plantation Forest	100.4	0.1544	Port & Harbor	0	0
Dry Shrub	74.64	0.1948	Transmigration Areas	16.89	0.911
Estate Crop	63.74	0.223	Mining Areas	0	0
Settlement Areas	2.8	0.8518	Open Swamp	0	0
Bare Ground	2.97	0.9217	Oil Palm	37	0.3
Savanna & Grasses	5.02	0.7788			

4.2 Annual emissions

Equation Two. Annual emissions from sugarcane production and use.

$$E_{annual} = (((GHG_{field} + GHG_{processing} + GHG_{Eprod} + GHG_{transport}) \times (C \times F)) + (GHG_{peat} \times A_{p)} - (GHG_{FS} \times Q_{p,y})) \pm (GHG_{peat} \times U_p \times A_p)$$

E_{annual}	= annual emissions from producing sugarcane-based bioethanol ($tCO_2e\ yr^{-1}$)
GHG_{field}	= GHG emissions from sugarcane cultivation growth ($kgCO_2e\ kg\ cane^{-1}$)
$GHG_{processing}$	= GHG emissions from sugarcane processing ($kgCO_2e\ kg\ cane^{-1}$)
GHG_{Eprod}	= GHG emissions from ethanol production ($kgCO_2e\ kg\ cane^{-1}$)
$GHG_{transport}$	= GHG emissions from transportation from field to mill ($kgCO_2e\ kg\ cane^{-1}$)
C	= sugarcane produced ($kg\ cane\ yr^{-1}$)
F	= the conversion factor for converting kg to tons
GHG_{peat}	= yearly GHG emissions from peat drainage ($tCO_2e\ ha^{-1}\ yr^{-1}$)
A_p	= total peatlands converted (ha)
GHG_{FS}	= difference in emissions from switching from gasoline to bioethanol (tCO_2e)
$Q_{p,y}$	= the quantity of bioethanol production, p, in each given year, y (L)
U_p	= uncertainty percentage from peat drainage

Table 5. Emissions factors for sugarcane production and processing.

Process	Emissions Factor	Unit	Uncertainty	Source
Sugarcane Cultivation	38.92	$kgCO_2e\ kg\ cane^{-1}$	-	[7]
Sugarcane Processing	0.095	$kgCO_2e\ kg\ cane^{-1}$	-	[7]
Ethanol Production	5.58	$kgCO_2e\ kg\ cane^{-1}$	-	[7]
Transportation	.015	$kgCO_2e\ kg\ cane^{-1}$	-	[7]
Peat Drainage	57.63	$tCO_2e\ ha^{-1}\ yr^{-1}$	39.68%	[8-11]
Fuel Switching	-.003	$tCO_2e\ L^{-1}$	-	Based on [12,13]

5. Sugar Intensification

Three scenarios test sugar and molasses production levels under a range field and factory efficiency levels, while also testing use of key crops in other contexts and industries.

Table 6. Sugarcane intensification scenarios.

Scenario	Field Efficiency	Factory Efficiency	Molasses Exports	Ethanol for Industry
Baseline	66.78 tc/ha	7.4%	OECD-FAO projections	Held constant at 2023 levels
Intensification	Linear growth from BAU in 2025 to reach 80 tc/ha in 2035	Linear growth from BAU in 2025 to reach 11.2% in 2035	OECD-FAO projections	Held constant at 2023 levels
No export	Linear growth from BAU in 2025 to reach 80 tc/ha in 2035	Linear growth from BAU in 2025 to reach 11.2% in 2035	Linear decrease from 2025 to reach no exports in 2035	Linear decrease from 2025 to reach no diversion for industrial use in 2035

6. GCAM Modeling Post-Processing

Table 7. Share of refined liquids for transportation derived from oil versus diesel.

Transportation mode	Assumed oil share	Source
Car	83%	[14]
Mini Car	100%	[14]
Light and medium truck	66%	[15]
Large car and truck	80%	[15]
2W and 3W	100%	[15]
Shipping	100%	[15]
Aviation	100%	[15]

7. EV Growth Scenarios And Calculations

To determine the impact of EV expansion on gas demand, we adjusted vehicle stock estimates for 2030, assuming one-for-one replacement of internal combustion engine (ICE) LDVs with EV LDVs and ICE motorcycles with electric motorcycles, and then assessing the impact on gas demand (see Equation Three). For LDV calculations, we assume that 83% of LDVs run on gasoline,[14] with an average fuel economy of 8.1 L/100km,[16] while for motorcycles, we assume that nearly all units run on gasoline, with an average fuel economy of 1.8 L/100km.[12] Using VKT estimates for LDVs[14] and motorcycles,[12] adjusted to project to 2030,[17] alongside vehicle stock estimates,[18] we estimate baseline per-unit gasoline use in 2030. After determining this baseline, we subtract it from EV deployment under a range of stock growth scenarios.

Equation 3. Change in gas demand for motorcycles or cars under increased EV stock

$$\Delta Dg=(VKT \times VS \times VS_g \times eff) - (VKT \times ((VS \times VS_g) - EV) \times eff)$$

D_g	= annual gas demand for cars or motorcycles (L)
VKT	= average vehicle kilometers traveled (km yr^{-1})
VS	= total gas-based vehicle stock, units
EV	= EV vehicle stock growth between 2024-2030, units
VS_g	= share of vehicle stock powered by gas
eff	= fuel efficiency (km L^{-1})

In our study, we consider two scenarios, including a medium ambition uptake target based upon current policies, and an ambitious uptake target promulgated in legislation in 2019. The mid-range target uses estimates from the Indonesian Business Council baseline scenario, while the ambitious target uses the Government of Indonesia's EV deployment target, as articulated under Presidential Regulation 55 of 2019 on Electric Vehicles. For each scenario, we subtract the 2030 target from the EV deployment rate at the end of 2024 to determine deployment during our study period.

Table 8. Total EV stock on the road by year and source.

	2024	2023 Projections	
	IESR[19]	*Indonesian Business Council*[20]	*GOI Target*[21]
LDV EVs	71,411	.6 million	2 million
2W EVs	160,578	4 million	12 million

Bibliography

1. De Alban, J. D. T., Connette, G. M., Oswald, P. & Webb, E. L. Combined Landsat and L-Band SAR Data Improves Land Cover Classification and Change Detection in Dynamic Tropical Landscapes. Remote Sens. 10, 306 (2018).

2. Doblas Prieto, J. Optimizing SAR data processing and thresholding for forest change detection: an application for early deforestation warnings on eastern Amazonia. (2020).

3. Lou, J. et al. Indonesia's land use dilemma: Balancing food security, bioenergy expansion, and deforestation risks. Preprint at https://doi.org/10.21203/rs.3.rs-6378393/v1 (2025).

4. Strategic Environmental Study: National Strategic Project for Sugar and Bioethanol Self-Sufficiency Development Area, Cluster 3, Merauke District, South Papua Province. https://drive.google.com/file/d/1ppdZDSB4RM44aRVujbVwxeWRJwbltBDR/view (2024).

5. Nusantara Atlas. Atlas of Deforestation and Industrial Plantations in Indonesia. Nusantara Atlas https://map.nusantara-atlas.org/ (2024).

6. Hansen, M. C. et al. Humid tropical forest disturbance alerts using Landsat data. Environ. Res. Lett. 11, 034008 (2016).

7. Khatiwada, D., Venkata, B. K., Silveira, S. & Johnson, F. X. Energy and GHG balances of ethanol production from cane molasses in Indonesia. Appl. Energy 164, 756–768 (2016).

8. Republic of Indonesia. National Forest Reference Level for Deforestation, Forest Degradation and Enhancement of Forest Carbon Stock. https://redd.unfccc.int/media/2nd_frl_indonesia_final_submit.pdf (2022).

9. Lam, W. Y. et al. Greenhouse gas footprints of palm oil production in Indonesia over space and time. Sci. Total Environ. 688, 827–837 (2019).

10. Carlson, K. M. et al. Carbon emissions from forest conversion by Kalimantan oil palm plantations. Nat. Clim. Change 3, 283–287 (2013).

11. van Beijma, S. et al. The challenges of using satellite data sets to assess historical land use change and associated greenhouse gas emissions: a case study of three Indonesian provinces. Carbon Manag. 9, 399–413 (2018).

12. Heidt, C., Jamet, M., Räder, D. & Weber, T. Greenhouse Gas Emissions of Transport and Reduction Potentials of BRT in Bandung, Pekanbaru and Semarang. https://www.changing-transport.org/wp-content/uploads/2020_GHG-of-Transport-and-Reduction-Potentials-of-BRT-in-Bandung-Pekanbaru-and-Semarang.pdf (2019).

13. Mera, Z. & Bieker, G. Comparison of the Life-Cycle Greenhouse Gas Emissions of Combustion Engine and Electric Passenger Cars and Two-Wheelers in Indonesia. https://theicct.org/publication/comparison-life-cycle-ghg-emissions-combustion-engine-and-electric-pv-and-2w-indonesia-sept23/ (2023).

14. Erahman, Q. F., Reyseliani, N., Purwanto, W. W. & Sudibandriyo, M. Modeling Future Energy Demand and CO2 Emissions of Passenger Cars in Indonesia at the Provincial Level. Energies 12, 3168 (2019).

15. IEA. An Energy Sector Roadmap to Net Zero Emissions in Indonesia. https://www.oecd.org/en/publications/an-energy-sector-roadmap-to-net-zero-emissions-in-indonesia_4a9e9439-en.html (2022) doi:10.1787/4a9e9439-en.

16. Fuel Economy in Indonesia. https://www.iea.org/articles/fuel-economy-in-indonesia (2021).

17. Syahputri, J., Suarga, E. B., Rahman, I., Zahari, T. N. & Ramdani, D. A. Impact of Air Pollution from the Transportation Sector on Health in Indonesia. https://lcdi-indonesia.id/wp-content/uploads/2024/03/2-EN-Policy-Note-2023.10.16.pdf (2023).

18. Number of Motor Vehicles by Province and Vehicle Type (units). BPS-Statistics Indonesia https://www.bps.go.id/en/statistics-table/3/VjJ3NGRGa3dkRk5MTlU1bVNFOTVVbmQyVURSTVFUMDkjMw==/number-of-registered-motor-vehicles-by-province-and-type-of-motor-vehicles--units-.html?year=2020.

19. Faris Adnan Padhilah et al. Indonesia Sustainable Mobility Outlook 2025: Driving Transport Decarbonization: Multi-Pathways to Sustainable Mobility in Indonesia. https://iesr.or.id/en/pustaka/indonesia-sustainable-mobility-outlook-ismo-2025/ (2025).

20. Indonesian Business Council Institute. Indonesia's EV Ecosystem in 2025: Progress and Regional Leadership Prospects. Indonesian Business Council Institute https://ibc-bulletin-vol4.vercel.app/ (2025).

21. President of Indonesia. Presidential Regulation Number 55 of 2019 on electric vehicles. Climate Change Laws of the World https://climate-laws.org/document/presidential-regulation-55-2019-on-electric-vehicles_411d (2019).